Tension-induced fusion of bilayer membranes and vesicles - Supplementary Information

Julian C. Shillcock and Reinhard Lipowsky
Max Planck Institute of Colloids and Interfaces
14424 Potsdam, Germany #

URL: http://www.mpikg.mpg.de/th/

The following pages contain supplementary information about the simulation method, the membrane model, and different aspects of membrane tension. Several time sequences of simulation snapshots, which display adhesion, hemifusion, fusion, and rupture, are also included as well as a table with the data underlying Figure 3 and 4 in the main text.

A. Dissipative Particle Dynamics Simulation Method

DPD was invented by Hoogerbrugge and Koelman[1] in 1992 and applied first to the calculation of the hydrodynamic drag on an array of cylinders in a moving fluid. The system reproduced the Stoke's behaviour of the drag coefficient with a few hundred particles. The algorithm was improved by Groot and Warren[2] in 1997, and their version is now in common use. Because the temperature control of the DPD thermostat is degraded for large time steps, we use a time step of $\delta t = 0.02$, for which the Groot-Warren integrator has been shown[3] to be as accurate as more complicated, self-consistent

schemes, and for which the temperature drift is less than 1% for all our simulations, including the 1.6 μs runs.

The elementary units in DPD are small volume elements called beads that represent either a number of identical molecules or molecular groups. Beads are considered to have internal degrees of freedom that have been integrated out, and that appear in the equations of motion as a pair of linked random and dissipative forces. These two forces act as a thermostat that keeps the system's kinetic temperature at a constant average value. Conservative forces between beads give them an identity and represent, for example, the hydrophilic and hydrophobic nature of some molecules. Once the forces are specified, beads evolve according to Newton's laws, and thermodynamic observables are measured as time averages over the bead coordinates as in Molecular Dynamics. DPD is distinct from MD in that the forces are soft, short-ranged, and represent a coarse-graining of the interactions of microscopic fluid elements rather than the inter-atomic potentials of MD. It is also distinct from Brownian Dynamics, which incorporates random forces between particles, because all forces in DPD conserve momentum.

B. Lipid Molecular Architecture and Membrane Physical Properties

Both the planar membrane and vesicle are composed of identical molecules. The rest of the simulation box, and vesicle interior, are filled with water particles, which represent clusters of water molecules, to an average density of 3 particles per unit volume. The simulation box size is $(72a_0)^3$, where a_0 is the bead diameter, and contains 1,100,000 beads of all kinds. A box containing only water particles under these conditions has

thermodynamic properties appropriate to water at room temperature[2]. The conservative interactions between the various bead types (hydrophilic lipid head, hydrophobic lipid tail and water) are described in detail in our previous work[4]. We mention here that the conservative forces are all linear in the bead-bead separation, as is almost universal in DPD simulations, and share the same cut-off distance a_0 that sets the length-scale in the simulations. The maximum repulsion at zero separation, a_{ij}, where the subscripts label the particle types, determines the degree of repulsion between bead types and takes the values aHH = aTT = aWW = 25, aHT = 50, aHW = 35, aTW = 75. These values are found to give well-ordered bilayers.

In Ref. 4, we measured quantitatively the equilibrium properties of a planar bilayer patch composed of lipids with a single hydrophobic tail. Such lipids do not make good constituents for vesicle simulations because the area stretch modulus is too large for lipids with 5 or more tail beads, and bilayers composed of lipids with 4 or less tail beads exhibit large shape fluctuations. Hence, in this work the vesicle and planar membrane are composed of model lipids containing three hydrophilic head beads, to which are attached *two* chains of four hydrophobic beads each. The tails are attached to adjacent head beads. Such lipids self-assemble to form a more robust membrane than the single-tailed lipids. A typical fusion event contains around 11,000 lipids in the vesicle and planar membrane combined. Although natural membranes contain a multitude of different types of lipid, and their presence may be important for fusion *in vivo*, artificial vesicles composed of a single type of lipid also fuse. Furthermore, from a conceptual point of view, it is

desirable to first understand the fusion of single-component membranes before one tackles the fusion of multi-component ones.

Comparing the equilibrium area per molecule for a typical lipid vesicle to that obtained in the simulations fixes the simulation length scale so that one bead diameter is $a_0 = 0.7$ nm. This is also the size of the beads in all the images presented. The average membrane thickness is 3.3-3.5 nm, comparable to that for dimyristoylphosphatidylcholine vesicles. The simulation time-scale is 0.016 nanoseconds/step, and is obtained by equating the diffusion coefficient of the lipids in the planar membrane to a typical experimental value of 5 μm^2/sec. Both the vesicle and planar membrane are in the fluid state, and can be placed under tension by changing the area-to-volume ratio and projected area, respectively.

C. Membrane Tension

The initial stage of our fusion protocol requires a vesicle and planar membrane to be created in states subject to uniform, global tensions. This is achieved simply by placing the appropriate number of molecules in the aggregates and allowing them to relax. The two aggregates must be placed close together, with a solvent-filled gap of less than 1.5 nm between their outer surfaces, in order for fusion to occur; larger separations result in no contact on the time scale of several microseconds. Indeed, for larger separations, the vesicle must first diffuse towards the membrane patch, a process which we don't want to study here.

The variation of the initial tensions represent the simplest protocol in order to study the dependence of fusion on tension. It is also possible, using the simulation approach described here, to explore the effects of applied tensions which are localized in space and/or in time (J.C. Shillcock and R. Lipowsky, in preparation). In this supplementary information, we mention some results about a second fusion protocol in which we apply an additional, relatively small tension after the membranes have hemifused.
This is accomplished by reducing the conservative interaction between the lipid head beads so that they prefer to pack closer together, thereby increasing the exposure of the hydrophobic tails to the solvent and raising the surface tension.

The constitutive relation between the planar membrane's projected area and tension is shown in Fig. S1 from the relaxed state until the membrane ruptures. We have not explicitly measured the tension in the vesicle, but have used the tension/projected area relation obtained for the planar membrane to estimate the vesicle tension. This provides a lower bound as the vesicle curvature is expected to raise its tension above that of the planar membrane with the same area per molecule. We do not expect this to qualitatively alter our results. The axes in Fig. 3 are labelled with the area per molecule for both the vesicle and planar membrane as this is the more accurately known quantity. It may be converted into a tension using Fig. S1. A series of collages of typical outcomes (adhesion, hemifusion, successful fusion and vesicle rupture) at different points in the morphology diagram are shown in Fig. S2. The data set of outcomes for each vesicle/planar membrane tension combination used in the preparation of Figures 3 and 4 is given in Table S1.

C.1 Regime of Low Initial Tensions

In addition to our main aim of studying tension-induced fusion, which we observe only for relatively large initial tensions corresponding to the shaded region of the morphology diagram, Fig. 3, we have also explored the low-tension regime.

Figure S1 shows that the tensionless state of the planar membrane occurs for a projected area $A/Na_0^2 = 1.26$. Fig. S2 A shows the evolution of a system composed of a relaxed planar membrane and a relaxed vesicle with the same area per molecule, $A/Na_0^2 = 1.26$. It is apparent, in this case, that the vesicle only adheres to the planar membrane which proceeds to partially wrap its surface. Adhesion appears to be the dominant pathway when either, or both, of the vesicle and planar membrane have low tensions. Further collages in Fig S2 show the gradual change from adhesion as the dominant pathway, through hemifusion, in which the proximal leaflets of the vesicle and planar membrane merge while the distal leaflets remain largely discrete, to the fusion regime in which the high tensions lead to either fusion or rupture of one the aggregates.

We note that the membranes investigated here, while certainly more extensible than phospholipid bilayer membranes, have comparable critical area expansions to polymersomes composed of diblock copolymers. One surprising result of our simulations, viz., the absence of any fusion events that take longer than 350 ns, is due to the fact that the hemifused state is stabilized in the membrane geometry considered here. Thus, as the proximal monolayers of the vesicle and planar membrane merge, and a large number of molecules starts to move between the two aggregates, the tension decreases

continously. After a time, which we find to be of the order of 350 ns, there is no longer sufficient tension in the vesicle/planar membrane system to induce rupture or fusion pore formation and the aggregates stay in the hemifused state.

C2. Time Evolution of Tensions

The time evolution of the tensions can be directly deduced from the time evolution of the membrane shapes as shown in Figure 1 and 2 and in Figure S2. After the vesicle and the membrane patch have come into contact, we can distinguish three different types of membrane segments: the contact zone between vesicle and membrane patch, the outer part of the vesicle membrane which is not in contact with the membrane patch, and the outer part of the membrane patch which is not in contact with the vesicle. In each of these three membrane segments, we can have a different tension, denoted by Σ_{co} , Σ_{ve} , and Σ_{pa}, respectively.

If the system is in mechanical equilibrium, these three tensions must be balanced along the contact line, i.e., along the boundary of the contact zone where the three membrane segments come together (this terminology is borrowed from the context of wetting phenomena). In such a balanced situation, the shape no longer evolves with time and the outer part of the membrane patch is horizontal, i.e., parallel to the base area of the simulation box. In the latter situation, one can deduce two well-defined contact angles, θ_{co} and θ_{ve} : The contact angle θ_{co} represents the angle between the contact zone segment and a horizontal reference plane whereas the contact angle θ_{ve} represents the angle between this plane and the outer part of the vesicle membrane. The balance of the two

force components, which are tangential and normal to the horizontal plane, respectively, then leads to the two relations

$$\Sigma_{pa} = \Sigma_{co} \cos(\theta_{co}) + \Sigma_{ve} \cos(\theta_{ve})$$

and

$$0 = \Sigma_{co} \sin(\theta_{co}) + \Sigma_{ve} \sin(\theta_{ve}) .$$

On the other hand, as long as the system is not in mechanical equilibrium, the tensions and contact angles will change with time. This time evolution is clearly seen in the time sequence shown in Figure S2.A which corresponds to the adhesion process of two relaxed membranes. Inspection of this figure shows that the contact angle θ_{ve} continuously decreases after about 112 nanoseconds until it reaches a constant value after about 800 nanoseconds. Likewise, Figure 1 shows that the tensions for the hemifused states have relaxed after 640 nanoseconds whereas Figure S2.B shows another hemifusion event in which the tensions change continuously between 160 and 480 nanosecondes. In general, the time evolution of the tensions will depend both on the intial tension, i.e., on the initial molecular areas, and on the total membrane areas which are initially stretched. The time evolution of the various tensions may be also estimated, at least in a qualitative fashion, by monitoring the membrane thickness: those membrane segments which experience a larger tension have a smaller thickness.

C.3 Fusion Protocol with Additional Tension

We have examined more closely the attempted fusion of a vesicle with a molecular area of $A/Na_0^2 = 1.3$ and a planar membrane with $A/Na_0^2 = 1.9$ (see Figures S2 B and C for a typical failed fusion outcome and a successful fusion event at this tension combination.)

Only two fusion events are observed in 10 independent simulations of 1.6 μs each for these parameter values, but if a small *additional* tension is imposed on the planar membrane after the vesicle has started to adhere to it, approximately 50% of the attempts result in successful fusion events.

D. Time Sequences of Snapshots

Time sequences of snapshots which illustrate the various pathways observed in the simulations are shown in Fig. S2 A) – E). These five simulation runs correspond to different points in the morphology diagram (Fig. 3 in the main text) which are characterized by different initial areas per molecule of the planar membrane and the vesicle. The initial molecular area in the planar membrane is denoted by X, the one in the vesicle by Y. Thus, each time sequence corresponds to a point with coordintates (X,Y) in the morphology diagram. Solvent particles initially outside the vesicle are invisible for clarity. Note that except in the case of vesicle rupture only a few tens of solvent particles initially inside the vesicle leak out prior to fusion: this is a neglible fraction of the ~50,000 initially inside. Also note that solvent particles that cross the boundaries of the simulation box reappear on the opposite side due to the periodic boundary conditions. Finally, note the different time scales for the sequences of snapshots.

E. Movie

The associated movie shows a typical fusion event and represents 320 ns of simulation time. The planar membrane patch and vesicle have initial molecular areas A/N = 1.95

and 1.35 respectively, and contain 5315 and 6105 lipids. For nearby values of the initial molecular areas, the membranes may also rupture as shown in Figure S2.E.

References

1. Hoogerbrugge, P. J. & Koelman, J. M. V. A. Simulating microscopic hydrodynamic phenomena with dissipative particle dynamics. *Europhys. Lett.* **19**, 155-160 (1992).

2. Groot, R. D. & Warren, P. B. Dissipative particle dynamics: bridging the gap between atomistic and mesoscopic simulation. *J. Chem. Phys.* **107**, 4423-4435 (1997).

3. Nikunen, P., Karttunen, M. & Vattulainen, I. How would you integrate the equations of motion in dissipative particle dynamics simulations? *Comp. Phys. Comm.* **153**, 407-423 (2003).

4. Shillcock, J. C. & Lipowsky, R. Equilibrium structure and lateral stress distribution of amphiphilic bilayers from dissipative particle dynamics *J. Chem. Phys.* **117**, 5048-5061 (2002).

Figures

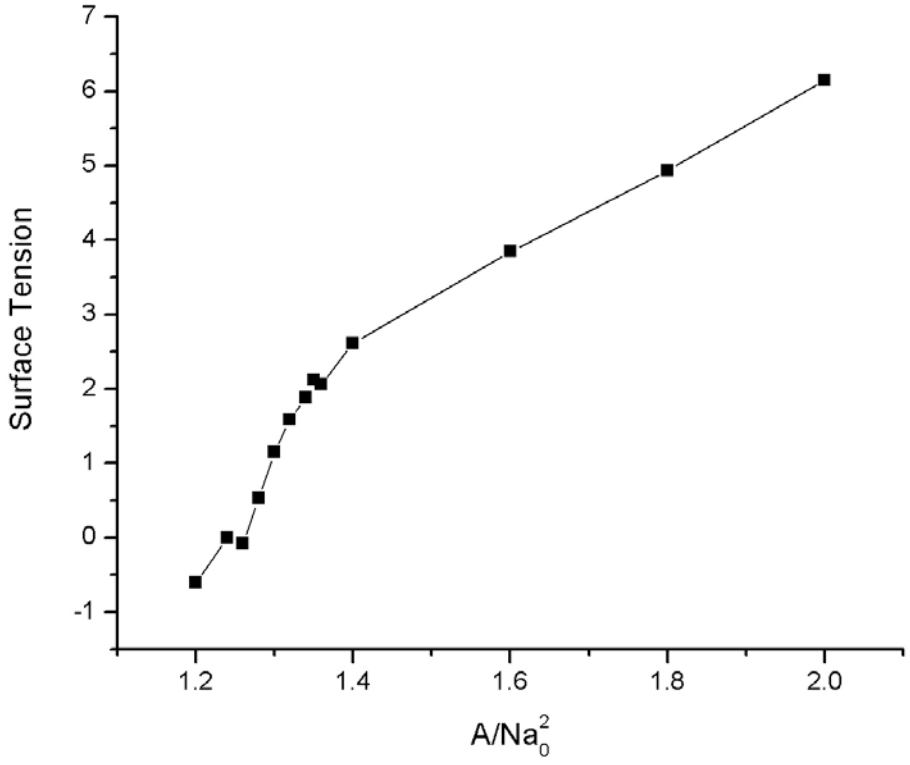

Fig. S1: Typical surface tension curve of the planar membrane against its projected area per molecule. The tensionless state occurs near $A/Na_0^2 = 1.26$ and the membrane ruptures almost immediately above $A/Na_0^2 = 2.0$. The surface tension is measured using the procedure described in Ref. 4. Note that there are two approximately linear regions for $A/Na_0^2 = 1.26 – 1.4$ and $1.5 – 2.0$. These regions can be used to convert the projected area into a tension value.

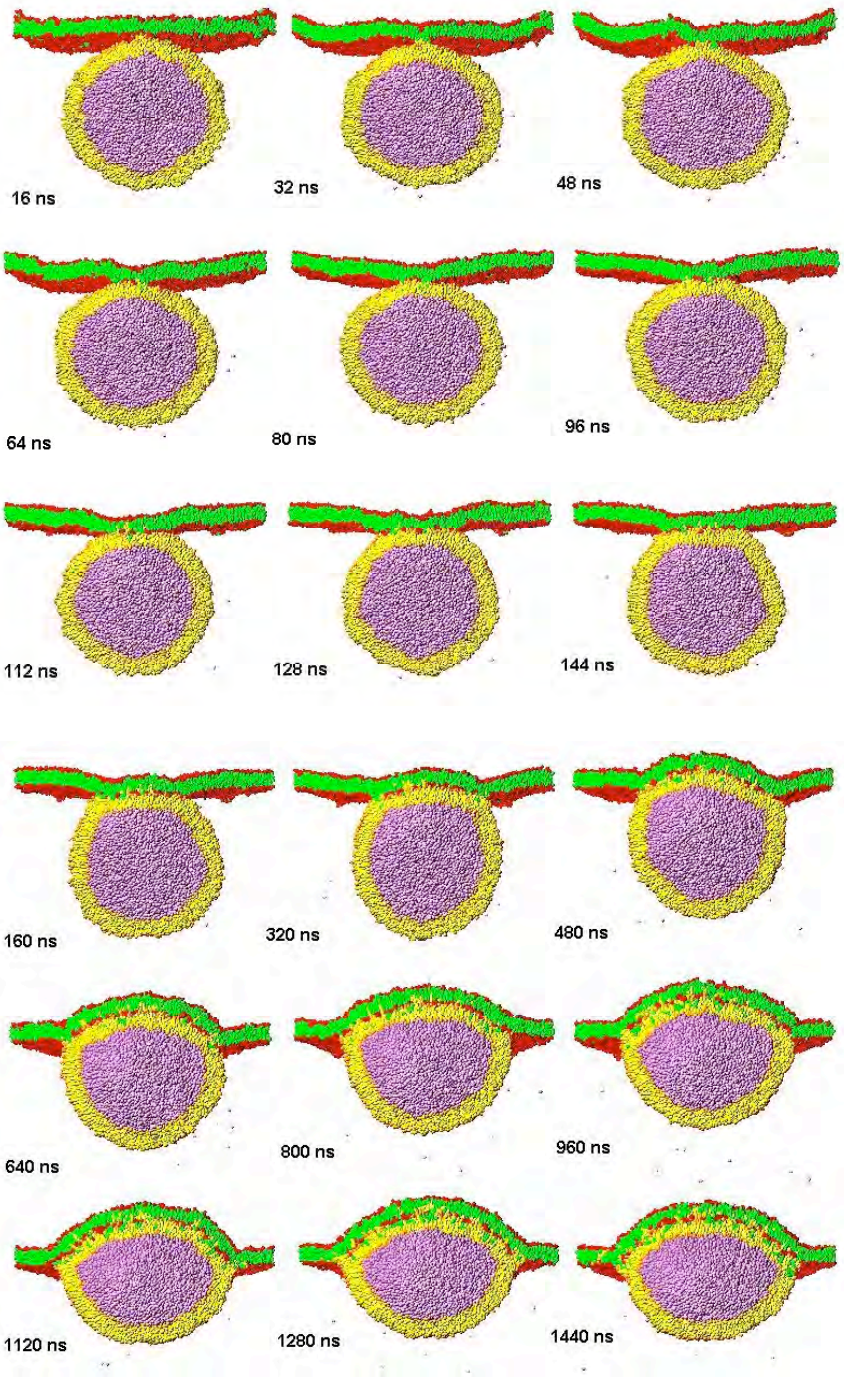

Fig. S2.A) Adhesion of a relaxed vesicle to a relaxed planar membrane, both of which have $A/Na_0^2 = 1.26$; this corresponds to the lower left corner (X,Y) = (1.26, 1.26) of

the morphology diagram. The first sequence of snapshots shows the initial contact between the vesicle and planar membrane up to 144 ns. The second sequence show the subsequent growth of the adhesion zone, and wrapping of the planar membrane around the vesicle, out to 1440 ns. Note the different time intervals between the snapshots in each panel.

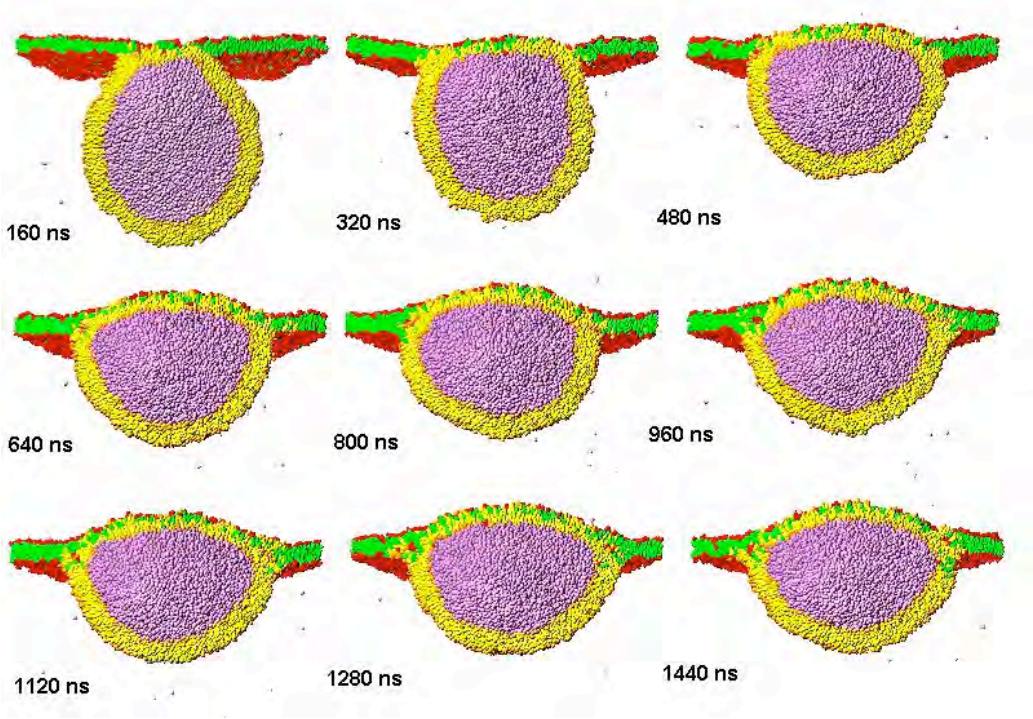

Fig. S2.B) Hemifusion event with molecular areas (X, Y) = (1.9, 1.3); this corresponds to the lower right part of the shaded fusion regime within the morphology diagram.

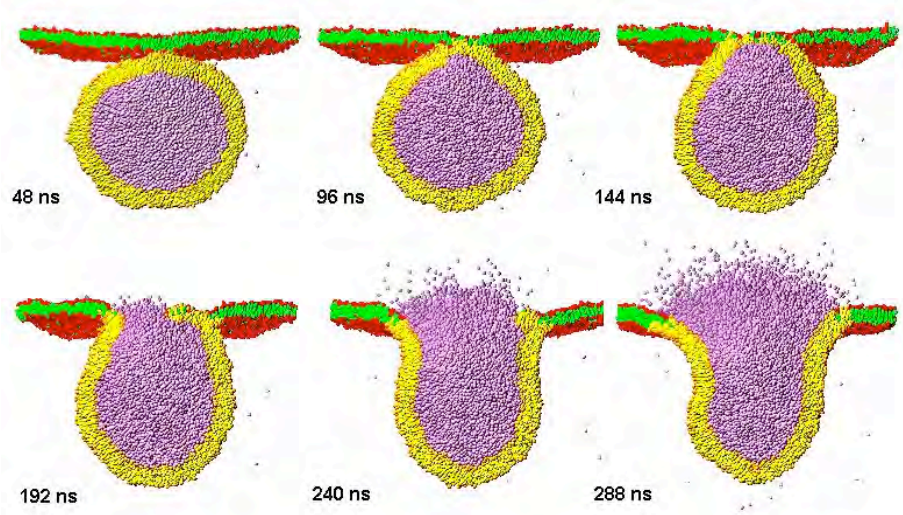

Fig. S2.C) Successful fusion event with (X, Y) = (1.9, 1.3); this corresponds to the same point in the morphology diagram as Fig. S2 B, but only 2 out of 10 independent runs resulted in fusion for this planar membrane/vesicle tension combination.

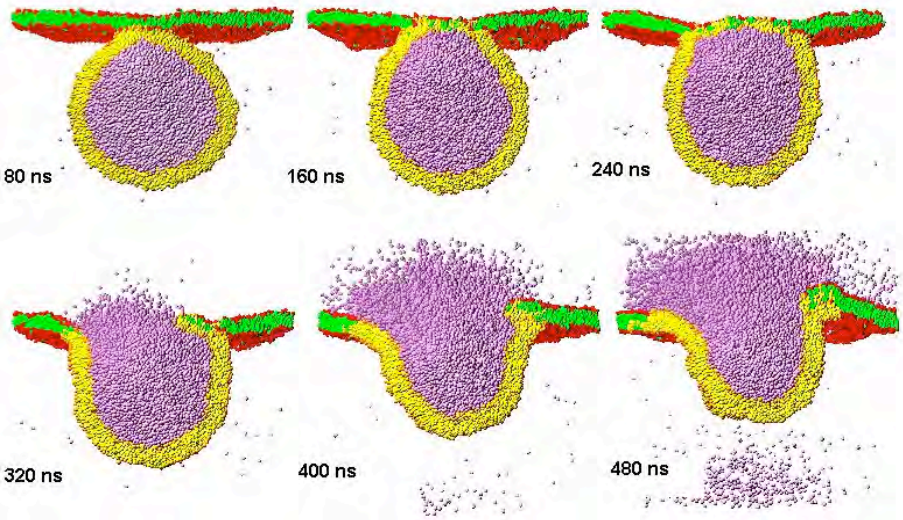

Fig. S2.D) Successful fusion event with (X, Y) = (1.8, 1.45); this corresponds to the upper left part of the shaded fusion regime within the morphology diagram.

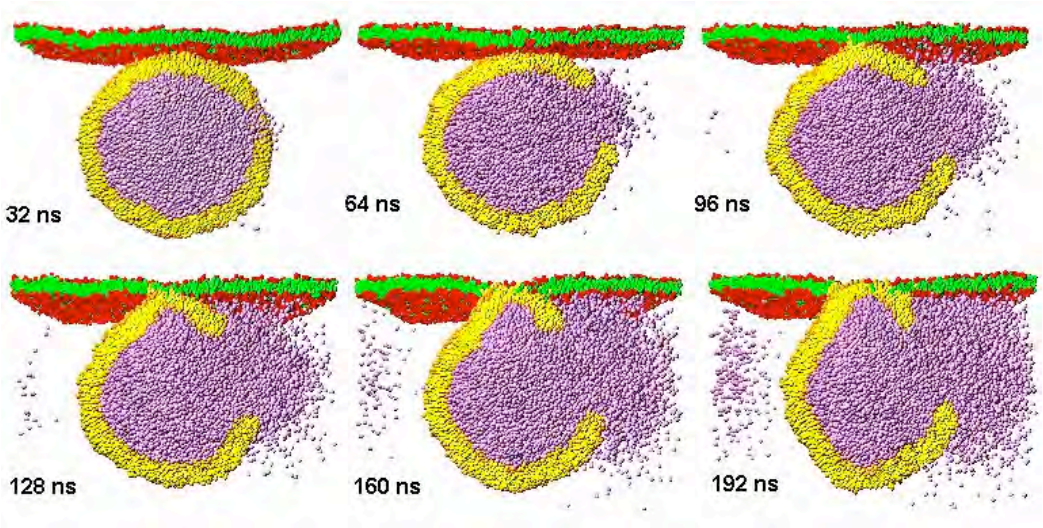

Fig. S2.E) Vesicle rupture event with (X, Y) = (1.95, 1.45); this corresponds to the upper right part of the shaded fusion regime within the morphology diagram

A/Na_0^2	**1.6**	**1.65**	**1.7**	**1.75**	**1.8**	**1.85**	**1.9**	**1.95**
1.45				13,14(2) HF,VR(3)	15,20	14, VR(2)	10(2),13.5,15, VR	10,11,14, VR
1.4	AD, HF	AD, HF	HF(4)	20, HF(5)	14,15, HF(2),VR	10,15,19	11,12,15(2)	11,15,17,21
1.35	AD, HF	HF(2)	HF(2)	HF(2)	13,19,20, HF(2)	HF	11,14,15,16, HF	10.5,11(2), 12,14,PR
1.3			HF		HF	HF	11,13,PR, HF(7)	15,PR, HF(2)

Table S1. Fusion times (in units of 1000 simulation steps or 16 ns) for successful fusion attempts, and alternative outcomes, organised according to the planar membrane (abscissa) and vesicle (ordinate) initial areas per molecule. The naming scheme for non-fusion outcomes is as follows: AD = vesicle adheres to the planar membrane; HF = vesicle and planar membrane hemifuse; PR = planar membrane ruptures prematurely; VR = vesicle ruptures prematurely. The numbers in brackets after an outcome are the number of times that outcome occurred at the given point in the morphology diagram. This data forms the basis of Figures 3 and 4, but note that the vesicle adhesion event for initally tensionless membranes with $A/Na_0^2 = 1.26/1.26$ shown in Fig. S2.A is not included here.